Journal of Alloys and Compounds 509 (2011) 5206–5210

Contents lists available at ScienceDirect

Journal of Alloys and Compounds

journal homepage: www.elsevier.com/locate/jallcom

Crystal structure peculiarity and magnetic behavior of $R_2Cu_{4-x}Sn_{5+x}$ (R = Gd, Tb, and Dy) compounds

V.V. Romaka[a,*], D. Gignoux[b], L. Romaka[c], N. Skryabina[d], D. Fruchart[b], Yu. Stadnyk[c]

[a] Department of Materials Engineering and Applied Physics, Lviv Polytechnic National University, Ustyyanovycha Str. 5, 79013, Lviv, Ukraine
[b] Institut Néel, CNRS, BP 166, 38042 Grenoble Cedex 9, France
[c] Department of Inorganic Chemistry, Ivan Franko Lviv National University, Kyryl and Mephodiy Str. 6, 79005, Lviv, Ukraine
[d] Perm State University, 15 Bukireva, 614990, Perm, Russia

ARTICLE INFO

Article history:
Received 10 January 2011
Received in revised form 9 February 2011
Accepted 9 February 2011
Available online 16 February 2011

Keywords:
Stannides
Crystal structure
Electronic structure
XRPD analysis
DSC analysis
Magnetic properties

ABSTRACT

The $Gd_2Cu_3Sn_6$, $Tb_2Cu_{3.5}Sn_{5.5}$, and $Dy_2Cu_{3.5}Sn_{5.5}$ intermetallic compounds were prepared by arc melting, annealed at 670 K and characterized by XRPD and DSC analyses. Rietveld refinement showed that they crystallize in tetragonal $Sm_2Cu_4Sn_5$ structure type (space group *I*4*mm*). The magnetic properties were studied in the temperature range 2–300 K and showed that in the paramagnetic state all studied compounds are Curie–Weiss paramagnets, among them $Tb_2Cu_{3.5}Sn_{5.5}$ and $Dy_2Cu_{3.5}Sn_{5.5}$ order antiferromagnetically at low temperatures and exhibit a metamagnetic transition. Electronic structure calculations were performed to evaluate chemical bonding.

1. Introduction

Two series of the ternary compounds with high tin content were found in most of the rare earth-copper–tin systems, i.e. $RCu_{1-x}Sn_{2-y}$ ($CeNiSi_2$-type, R – La–Sm) [1,2] and $R_2Cu_4Sn_5$ ($Sm_2Cu_4Sn_5$-type, R – Pr, Sm, Gd, and Tb) [2–4]. Both structure types contain the fragments of the binary AlB_2 and $BaAl_4$ structures ($CeNiSi_2$-type) or CaF_2, α-Po and $BaAl_4$ structures ($Sm_2Cu_4Sn_5$-type), staking along one direction (*Z*) and forming homologous series of the long periodical structures. In the {Pr, Nd}–Cu–Sn systems also the $PrCu_{0.25}Sn_{1.25}$ phase crystallized with AlB_2-type [2] and phase named τ_8 ($\sim Nd_4CuSn_5$) related to AlB_2-type [5] were previously known to exist. Magnetic properties were studied previously for the series of the $R_2Cu_4Sn_5$ intermetallics, where R is Pr, Sm, Gd, and Tb in the temperature range from 78 to 293 K [2,4], and it was indicated that stannides with Pr, Gd and Tb are Curie–Weiss paramagnets with effective magnetic moments closed to free R^{3+} ion values and negative paramagnetic Curie temperatures. In contrast, the magnetic susceptibility of the Sm compound does not follow Curie–Weiss law.

The aim of the present work is the investigation of the crystal structure and chemical bonding peculiarities of the $R_2Cu_{4-x}Sn_{5+x}$ tetragonal phases (R = Gd, Tb, and Dy) and their magnetic properties at the temperature ranging from 2 to 300 K.

2. Experimental

The alloys were prepared by weighing the stoichiometric amounts of Gd, Tb, and Dy metals (purity 99.9 wt.%), Cu metal (purity 99.99 wt.%), and Sn metal (purity 99.999 wt.%) and followed arc-melting the charges under purified, Ti-gettered, argon atmosphere with non-consumable tungsten electrode on a water-cooled copper hearth. The ingots were sealed in evacuated silica ampoules then annealed at 670 K for 720 h and subsequently quenched in ice water. The obtained samples were examined by scanning electron microscopy (SEM) using JEOL-840A scanning microscope. The phase analysis and crystallographic parameters of the samples were performed using X-ray powder patterns recorded with HCZ-4A (Cu Kα) and Bruker D8 (Cu $K\alpha_1$) powder diffractometers. The determination of the lattice parameters and the crystal structure refinements were performed using the WinPLOTR program package [6].

The magnetic measurements of the $R_2Cu_{4-x}Sn_{5+x}$ samples were carried out in the magnetic fields up to 10 T and in the temperature range from 2 K to 300 K using an automated extraction magnetometer.

The DSC analysis (NETZSCH STA449C Jupiter device) was performed on $Gd_2Cu_3Sn_6$, $Tb_2Cu_{3.5}Sn_{5.5}$ and $Dy_2Cu_{3.5}Sn_{5.5}$ compounds to check the limit of temperature range. The samples were heated in argon atmosphere up to 770 K at a rate of 10 K/min.

The electronic structure calculations were performed in the framework of DFT using pseudopotential method (CPMD) with plane-wave basis set. For the exchange-correlation functional the LDA [7] with PZ [8] parameterization was used.

* Corresponding author.
E-mail addresses: romakav@yahoo.com, romakav@lp.edu.ua (V.V. Romaka).

0925-8388/$ – see front matter © 2011 Elsevier B.V. All rights reserved.
doi:10.1016/j.jallcom.2011.02.055

Table 1
Cell parameters, experimental details, atomic and isotropic displacement parameters (in 10^2 nm^2) for $Gd_2Cu_3Sn_6$, $Tb_2Cu_{3.5}Sn_{5.5}$ and $Dy_2Cu_{3.5}Sn_{5.5}$ compounds.

R	Gd	Tb	Dy
a, nm	0.44141(1)	0.44044(2)	0.43945(2)
c, nm	2.4950(1)	2.4854(1)	2.4759(2)
Radiation	Cu Kα$_1$	Cu Kα	Cu Kα$_1$
Instrument	Bruker D8	HZG-4a	Bruker D8
R_1	B = 0.11(7)	B = 0.36(3)	B = 0.13(4)
2*a* (0 0 *z*)	*z* = 0	*z* = 0	*z* = 0
R^2	*z* = 0.6793(2)	*z* = 0.6826(1)	*z* = 0.6820(2) B = 0.13(4)
2*a* (0 0 *z*)	B = 0.11(7)	B = 0.36(3)	
Cu1	*z* = 0.0938(7)	*z* = 0.0931(3)	*z* = 0.0907(5)
4b (0 1/2 *z*)	B = 1.22(15)	B = 1.38(6)	B = 0.85(8)
Cu2	*z* = 0.2407(5)	*z* = 0.2413(8)	*z* = 0.2402(3)
2a (0 0 *z*)	B = 1.22(15)	B = 1.38(6)	B = 0.85(8)
Sn1	*z* = 0.2930(3)	*z* = 0.2807(2)	*z* = 0.2782(2)
4b (0 1/2 *z*)	B = 0.78(4)	B = 1.45(2)	B = 0.61(2)
Sn2	*z* = 0.4040(3)	*z* = 0.3971(2)	*z* = 0.3958(2)
4b (0 1/2 *z*)	B = 0.78(4)	B = 1.45(2)	B = 0.61(2)
Sn3	*z* = 0.5212(3)	*z* = 0.5241(1)	*z* = 0.5226(2)
2a (0 0 *z*)	B = 0.78(4)	B = 1.45(2)	B = 0.61(2)
(Cu/Sn)	*z* = 0.1399(3)	*z* = 0.1391(2)	*z* = 0.1415(3)
2a (0 0 *z*)	B = 0.78(4)	B = 1.38(7)	B = 0.85(8)
	Occ. = 1(Sn)	Occ. = 0.50/0.50	Occ. = 0.50/0.50
R_p	0.035	0.028	0.039
R_{wp}	0.032	0.037	0.051
R_{Bragg}	0.063	0.082	0.090

3. Results and discussion

3.1. Crystal structure and chemical bonding

At first, a new $Sm_2Cu_4Sn_5$ structure type was reported in Ref. [3], and the isotypic compounds were found also with Pr, Gd, and Tb [4]. Later, during investigation of the Nd–Cu–Sn system the new phase at corresponding compositions was found at 670 K, and performed crystal structure calculations showed some deviation from $Nd_2Cu_4Sn_5$ formula toward high Sn content – $Nd_2Cu_3Sn_6$, with occupation one of the 2*a* site for Cu atoms in starting model by (0.06Cu + 0.94Sn) mixture [5]. In Ref. [9] for the phase $Pr_2Cu_4Sn_5$ a slightly different composition and new formula $Pr_2Cu_3Sn_6$ was found on the basis of the microprobe data.

Detailed investigation of the Dy–Cu–Sn ternary system allowed us to find at 670 K the new ternary compound at $Dy_{18}Cu_{27}Sn_{50}$ composition [10]. The powder pattern of the $Dy_{18}Cu_{27}Sn_{50}$ alloy was successfully indexed on the basis of a tetragonal lattice with cell parameters a = 0.43945(2) and c = 2.4759(2) nm. The crystal structure refinements were performed on $Dy_{18}Cu_{27}Sn_{50}$ sample using the starting model of the $Sm_2Cu_4Sn_5$ structure type (space group *I*4*mm*). The final atomic and isotropic displacement parameters are listed in Table 1. The refinements of the site occupancies showed that one of the 2*a* positions for Cu atoms is occupied by (0.50Cu/0.50Sn) mixture. Thus, the chemical formula of the compound should be written as $Dy_2Cu_{3.5}Sn_{5.5}$, and it is in good agreement with the microprobe data. The model of the $Dy_2Cu_{3.5}Sn_{5.5}$ structure is presented in Fig. 1.

With regard to the various occupancy one of the 2*a* sites by (Cu/Sn) mixture for Nd and Dy compounds, it was decided also to perform the detailed crystal structure calculation for Gd and Tb compounds. The final atomic and isotropic displacement parameters of Tb compound are presented in Table 1, and the chemical formula of this compound, according to Rietveld refinement data, can be expressed as $Tb_2Cu_{3.5}Sn_{5.5}$. The refinements of the site occupancies of Gd compound showed that one of the 2*a* positions for Cu atoms in starting model is occupied exclusively by Sn atoms and the chemical formula of the compound should be written as $Gd_2Cu_3Sn_6$, and it is in good agreement with the microprobe analysis showing for this phase a composition richer in tin. Thus, the feature of these compounds is the structure peculiarity in occupancy of 2*a* site by mixture (Cu/Sn) with various compositions depending on rare earth atoms. The analysis of the interatomic distances in $Gd_2Cu_3Sn_6$, $Tb_2Cu_{3.5}Sn_{5.5}$ and $Dy_2Cu_{3.5}Sn_{5.5}$ compounds showed that the distance Sn1–Sn2 (0.2888, 0.2893, and 0.2912 nm for Gd, Tb, and Dy, respectively), Cu2–Sn3 (0.2810, 0.2790, and 0.2770 nm), Cu2–(Cu,Sn) (0.2471, 0.2482, and 0.2532 nm) and Sn1–(Cu,Sn) (0.2420, 0.2410, and 0.2390 nm) are shorter than the sum of the respective atomic radii (r_a(Sn) = 0.162 nm, r_a(Cu) = 0.127 nm), but it is almost equal to the sum of their covalent radii (r_c(Sn) = 0.141 nm, r_c(Cu) = 0.117 nm). Thus, crystal chemical analysis and electronic structure calculations showed that $R_2Cu_{4-x}Sn_{5+x}$ (x = 0) intermetallic compounds are characterized by the presence of metallic and ion-covalent bonds, caused by the high content of Sn in compounds. However, high density of states at Fermi level and absence of energy gap indicates metallic type of conductivity. Such a contribution of the covalence into the bond may cause localization of the electron density between these atoms, which is shown in Fig. 2. It is also clear that Sn–Sn and Cu–Sn bonds are stronger than those with participation of rare-earth atoms, which is in a good agreement with crystal chemical analysis.

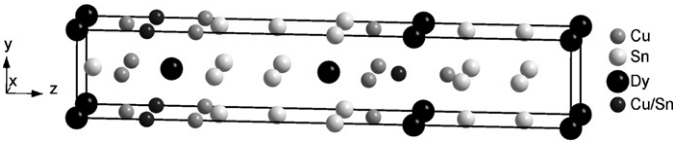

Fig. 1. The model of the $Dy_2Cu_{3.5}Sn_{5.5}$ structure.

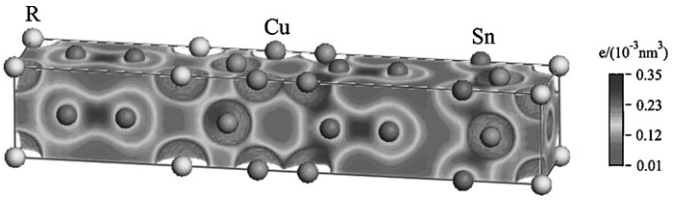

Fig. 2. The electron density distribution in $R_2Cu_{4-x}Sn_{5+x}$ (x = 0) compounds.

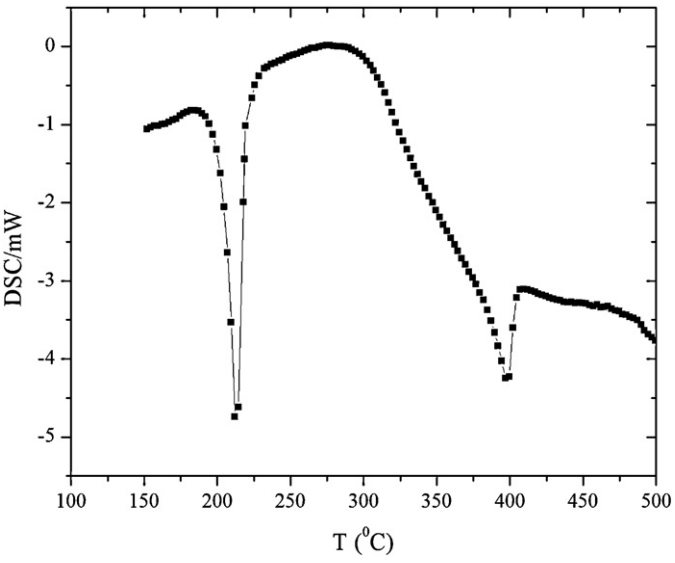

Fig. 3. DSC curve for the $Gd_2Cu_3Sn_6$ compound.

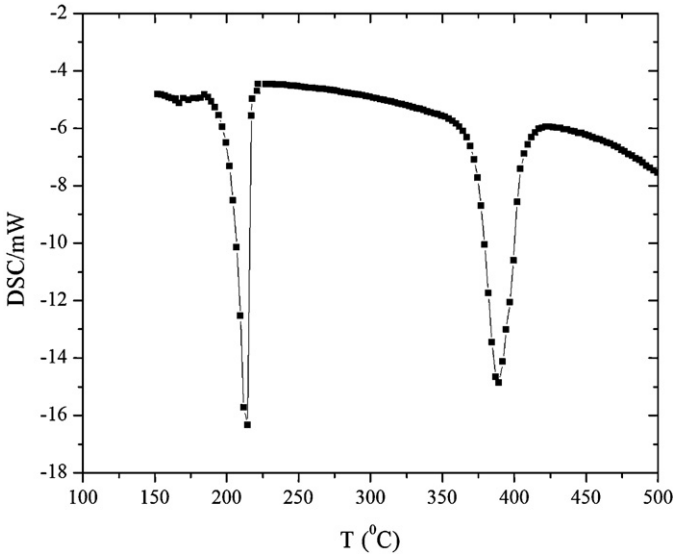

Fig. 4. DSC curve for the $Tb_2Cu_{3.5}Sn_{5.5}$ compound.

3.2. Differential scanning calorimetric analysis

Recently, we studied the component interactions in the Dy–Cu–Sn and Gd–Cu–Sn ternary systems at 670 K and 770 K and analyzed an influence of the heat treatment on the number of formed compounds [11,12]. The more remarkable difference at both studied temperatures is concerning to the $R_2Cu_{4-x}Sn_{5+x}$ phases, existed at 670 K, while at 770 K they were not observed. Thus, we checked $R_2Cu_{4-x}Sn_{5+x}$ compounds using the differential scanning calorimetric analysis and obtained results confirmed the limited temperature ranging for those phases, showing the thermal induced transitions for $Gd_2Cu_3Sn_6$, $Tb_2Cu_{3.5}Sn_{5.5}$ and $Dy_2Cu_{3.5}Sn_{5.5}$ compounds at 398.1, 389.6, 404.2 °C and 213.4, 213, 217.5 °C, respectively, which can be associated with the formation of the corresponding phases and their next decomposition, respectively (Figs. 3–5). Obtained results confirmed the limited temperature range for the compounds with Sn content higher than 50 at.% in the {Gd, Tb, Dy}–Cu–Sn systems. This fact is in a good agreement with the binary Cu–Sn system [13], which is characterized by low temperature formation of the binary phases in the region more than 50 at.% Sn and by the presence of liquid at low temperature. The presence of Sn bubbles is clearly observed in $Gd_2Cu_3Sn_6$ sample heated at 770 K (Fig. 6).

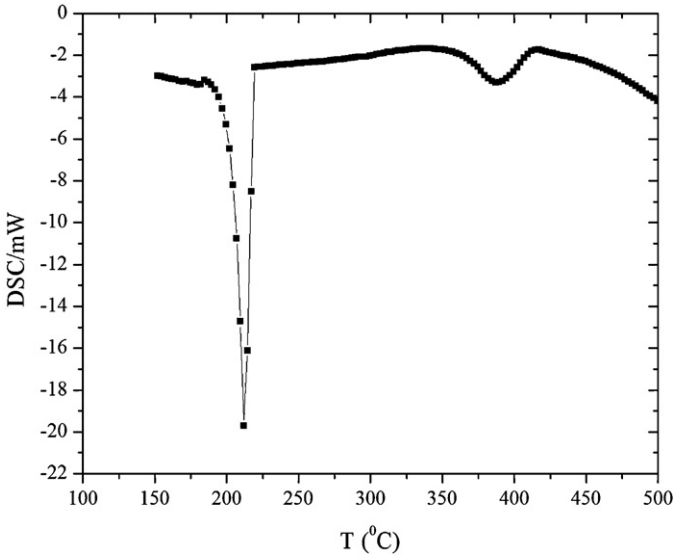

Fig. 5. DSC curve for the $Dy_2Cu_{3.5}Sn_{5.5}$ compound.

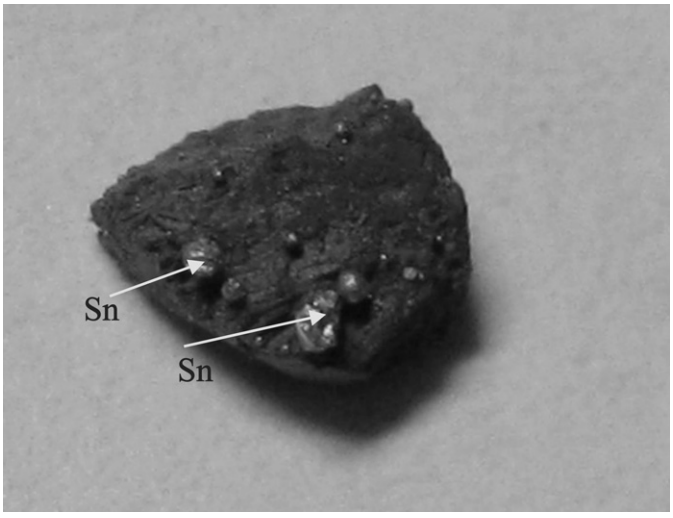

Fig. 6. The photograph of the $Gd_2Cu_3Sn_6$ sample heated at 770 K.

3.3. Magnetic properties

Magnetic behavior of the $R_2Cu_{4-x}Sn_{5+x}$ intermetallics was studied by magnetic susceptibility (χ) measurements in a magnetic field up to 0.1 T and in the temperature range 2–300 K (from χ^{-1}(T) dependences the effective magnetic moments μ_{eff} and the paramagnetic Curie temperatures θ_p were calculated) and magnetization (M) measurements in magnetic fields up to 10 T and different temperatures (in order to get the value of the pseudo-saturated magnetic moment and the character of the magnetization plots). The temperature dependencies of the inverse magnetic susceptibility of the compounds $Gd_2Cu_3Sn_6$, $Tb_2Cu_{3.5}Sn_{5.5}$, and $Dy_2Cu_{3.5}Sn_{5.5}$, measured in a field of 0.1 T, are reported in Fig. 6. In the paramagnetic region, the magnetic susceptibility follows a Curie–Weiss law for all three compounds and only R^{3+} ions determine the magnetic

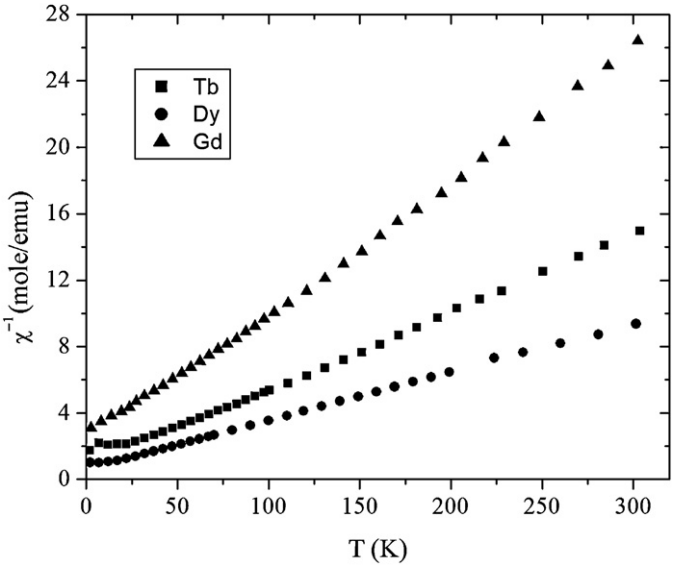

Fig. 7. Temperature dependencies of the inverse magnetic susceptibility for the $R_2Cu_{4-x}Sn_{5+x}$ compounds.

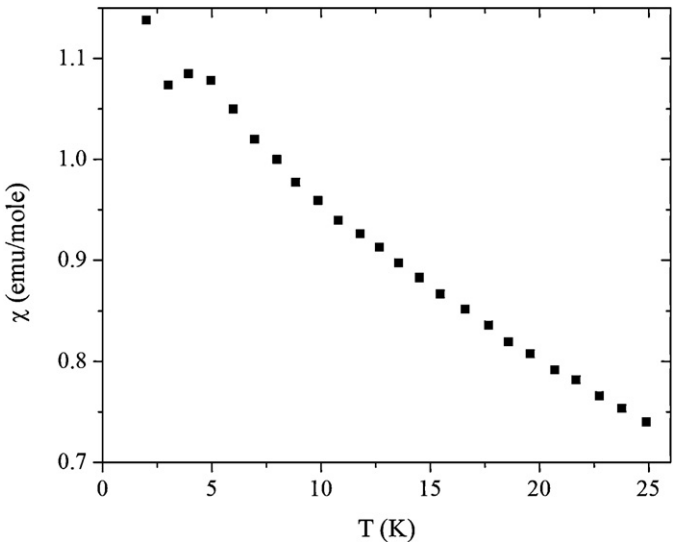

Fig. 8. Temperature dependence of the susceptibility of the $Dy_2Cu_{3.5}Sn_{5.5}$ compound at low temperatures.

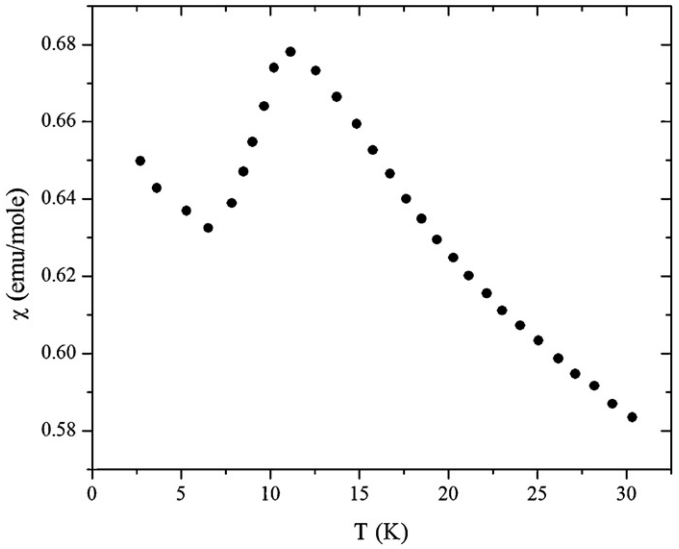

Fig. 9. Temperature dependence of the susceptibility of the $Tb_2Cu_{3.5}Sn_{5.5}$ compound at low temperatures.

behavior. Calculated effective magnetic moments per formula unit are close to the magnetic moment values of the respective free R^{3+} ions (see Table 2). For $Gd_2Cu_3Sn_6$ compound no magnetic ordering is observed up to 2 K, it is a Curie–Weiss paramagnet in all investigated temperature range as shown in Fig. 7. The magnetic characteristics of investigated compounds are given in Table 2.

The low temperature magnetic susceptibility of the $R_2Cu_{4-x}Sn_{5+x}$ compounds, where R = Tb, Dy, measured in a field of 0.1 T are reported in Figs. 8 and 9. For $Dy_2Cu_{3.5}Sn_{5.5}$, a pronounced maximum characteristic of an antiferromagnetic

Table 2
Magnetic characteristics of the $R_2Cu_{4-x}Sn_{5+x}$ compounds.

R	T_N (K)	θ_p (K)	$\mu_{eff}(\mu_B)$	
			Exp.	Theor.
Gd		−40.0	7.47(1)	7.94
Tb	12	−23.4	9.58(1)	9.72
Dy	4	−24.5	10.54(1)	10.65

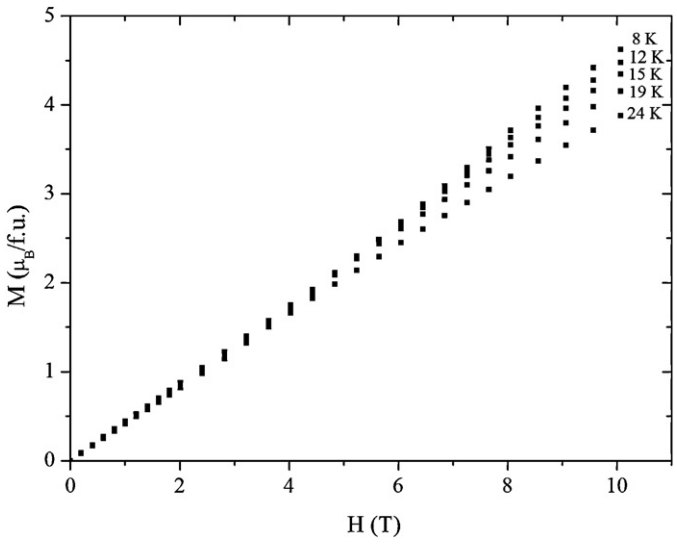

Fig. 10. Magnetization versus applied field at low temperatures for the $Tb_2Cu_{3.5}Sn_{5.5}$ compound.

ordering is observed at T_N = 4 K. For $Tb_2Cu_{3.5}Sn_{5.5}$ one also observes a maximum at T_N = 12 K but it is much more spread out than for the compound with Dy. This behavior is quite similar to that observed in the other Tb based stannides, $TbNi_3Sn_2$ [14] and $TbCo_xSn_2$ [15]. In order to more deeply study the magnetic behavior of the $Tb_2Cu_{3.5}Sn_{5.5}$ compound in this range, we have measured M(*H*) dependencies at different low temperatures (Fig. 10) closed to observed transition. It is clearly evidenced that measured behaviors at every temperatures are typical for Curie–Weiss paramagnetic materials.

The field dependencies of magnetization up to 10 T at different temperatures for all studied materials showed that the magnetic saturation is not reached in the maximum applied field of 10 T. Whereas, below T_N the $Tb_2Cu_{3.5}Sn_{5.5}$ and $Dy_2Cu_{3.5}Sn_{5.5}$ compounds exhibit a metamagnetic transition with a critical fields of about 3.1 T and 2.3 T at 2 K, respectively (Fig. 11).

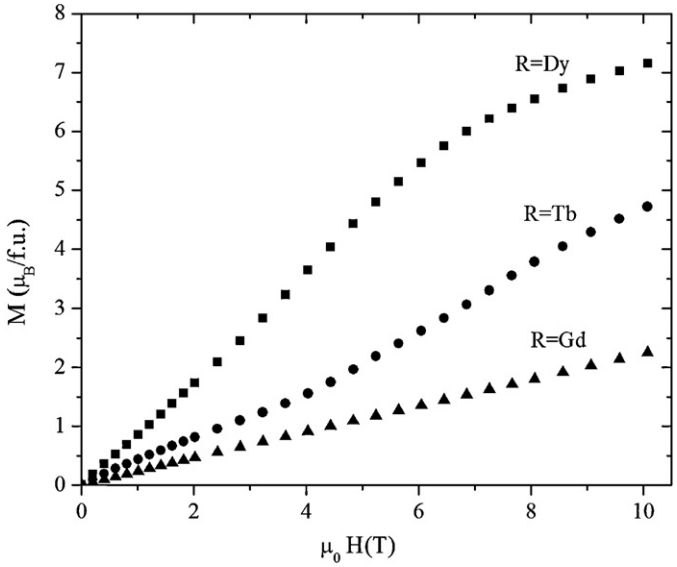

Fig. 11. Magnetization versus applied field at 2 K for the $Gd_2Cu_3Sn_6$, $Tb_2Cu_{3.5}Sn_{5.5}$ and $Dy_2Cu_{3.5}Sn_{5.5}$ compounds.

4. Conclusions

In conclusions, it should be noted that the series of the ternary compounds with general composition $R_2Cu_{4-x}Sn_{5+x}$ was studied by crystal structure and magnetic properties investigations. Performed in our work crystal structure analysis confirmed well a varied percentage of copper and tin atoms in *2a* atomic site, giving slightly different compositions for representatives of $R_2Cu_{4-x}Sn_{5+x}$ series. Electronic structure calculations showed strong interaction between Sn–Sn and Cu–Sn atoms resulted in electron density localization. Obtained results confirmed the limited temperature range for the compounds with Sn content higher than 50 at.% in the {Gd, Tb, Dy}–Cu–Sn systems. Counting the number of rare earth atoms according to calculated formula investigated compounds, we obtained a good agreement between the experimental values of μ_{eff} and the corresponding values for R^{3+} ions.

Acknowledgement

The work was supported by the Ministry of Ukraine for Education and Science.

References

[1] L. Komarovskaya (Romaka), S.A. Sadykov, R.V. Skolozdra, Ukr. J. Phys. 33 (8) (1988) 1249–1251.
[2] R.V. Skolozdra, in: K.A. Gschneidner Jr., L. Eyring (Eds.), Handbook on the Physics and Chemistry of Rare-Earths, vol. 24, North-Holland, Amsterdam, 1997 (chapter 164).
[3] R.V. Skolozdra, L.P. Komarovskaya, E.E. Terletskaya, L.G. Akselrud, Krystallograph 36 (2) (1991) 492–493.
[4] L. Komarovskaya, R.V. Skolozdra, Izv. AN USSR 2 (1992) 231–232.
[5] P. Riani, M.L. Fornasini, R. Marazza, D. Mazzone, G. Zanicchi, R. Ferro, Intermetallics 7 (1999) 835–846.
[6] T. Roisnel, J. Rodriguez-Carvajal, Materials Science Forum, Proceedings of the European Powder Diffraction Conference (EPDIC7), 2001, pp. 378–381, 118.
[7] L. Hedin, B.I. Lundqvist, J. Phys. C: Solid St. Phys. 4 (1971) 2064.
[8] J.P. Perdew, A. Zunger, Phys. Rev. B 23 (1981) 5048.
[9] P. Riani, D. Mazzone, R. Marazza, G. Zanicchi, R. Ferro, Intermetallics 8 (2000) 259.
[10] O.I. Bodak, V.V. Romaka, A.V. Tkachuk, L.P. Romaka, Yu.V. Stadnyk, J. Alloys Compd. 395 (2005) 113.
[11] V. Romaka, Yu. Gorelenko, L. Romaka, Visnyk Lviv Univ. 49 (2008) 3–9.
[12] L. Romaka, V.V. Romaka, E.K. Hlil, D. Fruchart, Chem. Met. Alloys 2 (2009) 68–74.
[13] T.B. Massalski, Binary Alloy Phase Diagr., ASM, Metals Park, OH, 1990.
[14] V.V. Romaka, D. Gignoux, D. Fruchart, L. Romaka, Yu. Gorelenko, J. Alloys Compd. 454 (2008) 5.
[15] A. Gil, E. Wawrzynska, J. Hernandez-Velasco, A. Szytuła, A. Zygmuntc, J. Alloys Compd. 365 (2004) 31.